GROWTH OF INDIUM GALLIUM NITRIDE BY METALORGANIC CHEMICAL VAPOR DEPOSITION AND SIMULATION FOR SOLAR CELL APPLICATION

TAN AIK KWAN

UNIVERSITI SAINS MALAYSIA

2025

GROWTH OF INDIUM GALLIUM NITRIDE BY METALORGANIC CHEMICAL VAPOR DEPOSITION AND SIMULATION FOR SOLAR CELL APPLICATION

by

TAN AIK KWAN

Thesis submitted in fulfilment of the requirements

for the degree of

Doctor of Philosophy

October 2025

DECLARATION

I hereby declare that this dissertation, submitted to Universiti Sains Malaysia as partial fulfilment of the requirement for the Doctor of Philosophy degree, has not been submitted to any Universities or Institutions for any degrees. I also declare that the work described herein is based on my original work, except for quotations and citations that have been duly acknowledged.

(Signed)

(TAN AIK KWAN)

ACKNOWLEDGEMENT

In my earlier career as a fresh graduate engineer, I always pondered the right path that could widen my global perspectives. After deep consideration, I decided to make a major switch to explore the optoelectronic field in my early twenties, which is deemed a more promising global market and demand. The INOR nitride materials research grabbed my attention, hence I took my first step to investigate further. As a person with a high level of curiosity, I started to read articles and literature regarding nitride material before officially raising the request to my respected supervisor, Assoc. Prof. Dr. Ng Sha Shiong regarding the InGaN solar cell project. Without his undivided attention and support, I might not have been able to gain knowledge of various high-end tools such as metalorganic chemical vapor deposition reactor, lithography, e-beam evaporator, and other exciting tools. This knowledge is a strong foundation for getting an earlier job placement before I officially graduate from the INOR. Next, I would like to express my gratitude to Kak Atiqah, Pn. Rahim, and En. Anas during my candidature. I would also like to thank my parents for supporting my decision and providing financial support at the beginning of my study, which was also the key period for me to proceed confidently. Of course, I will not forget Habib and Tian Kun, who were willing to share their knowledge and techniques for using analytic software, which was alien to me. Finally, I would like to thank the financial support from Universiti Sains Malaysia through the Research University Grant (Account No. 1001/CINOR/8011127).

"Life begins at the end of your comfort zone."

TABLE OF CONTENTS

LIST OF TABLES

Page

LIST OF FIGURES

Page

LIST OF SYMBOLS

a	Lattice constant of the crystalline structure
α	Absorption coefficient
b	Burgers vector length
β	XRD FWHM in arcsec
c	Lattice constant of the crystalline structure
D	Dislocation density
h	Planck's constant
hv	Photon Energy
h, k, l	Miller indices
θ	XRD theta angle
ω	XRD omega angle
Q	Reciprocal lattice point coordinate
T	Transmittance

LIST OF ABBREVIATIONS

AFM	Atomic force microscopy
Cp_2Mg	Bis(cyclopentadienyl)magnesium
FESEM	Field emission scanning electron microscopy
FSS	Flat sapphire substrate
FWHM	Full-width-at-half-maximum
HRXRD	High-resolution X-ray diffractometry
MBE	Molecular beam epitaxy
MOCVD	Metal-organic chemical vapor deposition
MQW	Multiple Quantum Wells
NRR	Non-radiative recombination
PL	Photoluminescence
QB	Quantum Barrier
QE	Quantum efficiency
QW	Quantum well
RC	Rocking curve
RMS	Root mean square
RSM	Reciprocal Space Mapping
SiH_4	Silane; Silicon hydride (IV)
SQW	Single Quantum Well
TEGa	Triethyl-gallium
TMAl	Trimethyl-aluminium

TMGa	Trimethyl-gallium
TMIn	Trimethyl-indium
UV-Vis	Ultraviolet-visible

PERTUMBUHAN INDIUM GALIUM NITRIDA DENGAN TEKNIK PEMENDAPAN WAP KIMIA LOGAM DAN SIMULASI UNTUK APLIKASI SEL SURIA

ABSTRAK

Indium gallium nitride (InGaN) digunakan untuk pelbagai aplikasi optoelektronik kerana ciri-ciri unik seperti jurang jalur tenaga terus dan boleh diselaras dari 0.64 eV sehingga 3.42 eV dengan mengubah komposisi indium. Tetapi, pembangunan peranti InGaN menghadapi cabaran seperti pertumbuhan filem nipis InGaN kristal berkualiti tinggi dengan komposisi indium tinggi serta bersifat jenis-*p*. Dalam kajian ini, fokus utama adalah pertumbuhan filem nipis InGaN dengan pemendapan wap kimia logam untuk komposisi indium (~20%) dengan kualiti kristal yang baik (FWHM < 2000) serta pengoptimuman syarat penyepuhlindapan untuk filem nipis yang didopkan dengan magnesium (Mg) yang berciri jenis-*p*. Pengoptimuman suhu pertumbuhan dan nisbah V/III menunjukkan filem nipis InGaN 300nm dengan komposisi indium maksimum 21.18% telah ditumbuhkan dan sampel terbaik menunjukkan kualiti kristal dengan lebar penuh pada separuh maksimum (FWHM) serendah 1975 dan 1746 untuk puncak belauan (0 0 0 2) dan (1 0 -1 5) dengan nisbah V/III 16562. Suhu penyepuhlindapan 650°C didapati mempunyai kerintangan dan ketumpatan kehel paling rendah untuk sample didopkan Mg. Akhirnya, kajian numerik bagi struktur sel suria homosambungan *p-i-n* menunjukkan peningkatan sebanyak ~0.60% melalui struktur penyerap bergred linear kerana lebih banyak tenaga foton yang ditangkap dengan menggunakan penyerap celah jalur lebar.

GROWTH OF INDIUM GALLIUM NITRIDE BY METALORGANIC CHEMICAL VAPOR DEPOSITION AND SIMULATION FOR SOLAR CELL APPLICATION

ABSTRACT

Indium gallium nitride (InGaN) is widely used for various optoelectronic applications due to its unique properties, such as a direct and tunable bandgap from 0.64 eV to 3.42 eV by varying the indium composition. However, the development of InGaN-based devices encountered difficulty in growing indium-rich and high-crystalline quality InGaN thin film as well as *p*-type InGaN thin film. In this study, the key focus will be the metalorganic chemical vapor deposition (MOCVD) growth of indium-rich (> 20%) InGaN thin film with good crystalline quality (FWHM < 2000) and the optimization of annealing conditions for the magnesium (Mg) doped InGaN thin film for the *p*-type behaviour. By optimizing the growth temperatures and V/III ratios, a 300 nm InGaN thin film with a maximum indium composition of 21.18% was successfully grown and the best sample showed good crystalline quality with full-width-at-half-maximum (FWHM) of 1975 and 1746 for (0 0 0 2) and (1 0 -1 5) diffraction peaks, respectively at the V/III ratio of 16562. Annealing temperature of 650°C to the Mg-doped InGaN thin films showed the lowest bulk resistivity and dislocation densities as compared with other annealing temperatures. Lastly, a numerical study of a homojunction *p-i-n* solar cell structure with an indium composition of 20% showed an improvement by ~0.60% via the linear graded absorber structure due to more photon energy captured by using a wider bandgap absorber.

CHAPTER 1 INTRODUCTION

1.1 Overview of the current solar energy demand

The global demand for renewable energy has been surging in recent years due to numerous influences such as climate change, energy security and access, strategic economic development, and public health concerns about the reliance on fossil fuels. In the year 2022, the Russia-Ukraine war has impacted the global reliance on autocratic regimes for energy supply. The war also brought out the concern of dependence on imported fossil fuels as the main source of energy supply, especially to European countries (Trypolska and Rosner, 2022). Eventually, the development of energy harvesting technologies without the usage of fossil fuels will become one of the critical fields for development.

Renewable energy is derived from naturally replenishing resources such as hydro power, solar, geothermal, wind, and bioenergy, where the utilization of these energies could generate electricity for daily usage (Ang *et al.*, 2022). From the analysis and forecast by the International Energy Agency (IEA), the global renewable capacity is expected to grow by 2.7 times by 2030, and nearly 140 countries have played their roles in supporting the climate and energy security policies to make renewable energy generation cost-competitive with fossil-fired power plants. In the electrical sector, the renewable energy share is expected to increase from 30% in 2023 to 46% in 2030, where solar and wind-based energy will exceed hydropower as the key renewable energy sources in 2030, as shown in Figure 1.1 (*Renewables 2024: Analysis and forecast to 2030*, 2024).

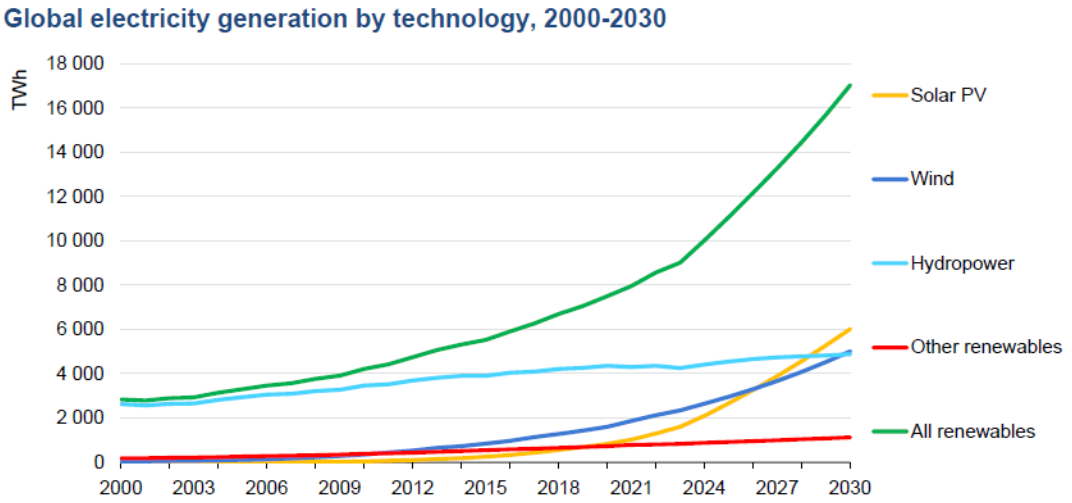

Figure 1.1: Global electricity generation by technology from 2000-2030 (*Renewables 2024: Analysis and forecast to 2030*, 2024)

Several factors were pinpointed to propel solar energy as the key electrical energy source, such as the abundance of sun radiation, versatility and scalability to deploy solar panels across diverse locations, low operating cost to maintain the solar energy farm, and minimal environmental impact for the installation. Next, the presence of big players such as China and India contributing to the manufacturing of solar panels boosted the usage of solar energy to become the main renewable energy source worldwide. From January – July 2024, the largest solar farm in China increased the number of solar panels by 28% as compared with the same period in 2023, whereas India expanded the solar capacity by 77% in the first 7 months of 2024 as compared to the same period in 2023. Similar behavior was also observed in the US, where an additional solar capacity of 55% in 2024 as compared to 2023 (Fulghum and Graham, 2024). Hence, it is concluded that solar panel technology is the cornerstone technology in supporting the renewable energy share, especially in countries near the equator such as Malaysia, Indonesia, Singapore, and Thailand.

Malaysia is located near the Earth's equator with at least 10 hours of sunlight exposure daily, which makes the country always hot and humid with a generous amount of rainfall all year round. The country is blessed with strong solar irradiance all year round with a monthly mean daily value of global solar radiation of ~18.0 MJ/m^2/day and a monthly average isolation clearness index of 0.45 to 0.55 (Mohammad *et al.*, 2020; Vaka *et al.*, 2020). The abundance of solar radiation makes Malaysia a potential country for the large-scale implementation of solar technology. In December 2021, the Ministry of Energy and Natural Resources (KetSA) and the Sustainable Energy Development Authority (SEDA) Malaysia launched the Malaysia Renewable Energy Roadmap (MyRER) to outline a strategic framework to decarbonize Malaysia's electricity sector. The roadmap targeted a 31% renewable energy share in the national installed capacity mix by 2025 (12916 MW) and 40% by 2035 (17996 MW) to support Malaysia's climate goals, such as a 45% reduction in greenhouse gas emissions. Solar energy is specifically being recognized by MyRER as one of the strategic pillars with a total solar energy capacity of 269 GW, which includes 210 GW from ground-mounted systems, 42 GW from rooftop solar panels, and 17 GW from floating solar systems. This makes up the second-largest renewable energy source after hydropower. Different key strategies such as the Net Energy Metering (NEM) program and Large-Scale Solar (LSS) auctions accelerate the tariff review, capacity limit removal, and so on. New business models and technology expansion have been gradually moving forward to explore innovative solutions to optimize solar energy capacity in Malaysia (Rahman, Imteyaz, and Aroua, 2023).

1.2 Overview of solar cell technology and its status

The solar cell is based on the photovoltaic (PV) effect to convert sunlight into electrical energy, where the PV effect can be broken down into several key stages to convert the photon energy from sunlight into electricity. The first stage of the PV effect starts with light absorption, where the photons with varying energy from the sun strike the solar cell's semiconductor material. Photons with energy equivalent to or greater than the bandgap energy of the semiconductor material will be absorbed to excite the electrons from the valence band to the conduction band. In the second stage of the PV effect, the energy from photons will be used in the electron-hole pair generation, where the electrons free themselves from their atoms to form charged carriers (Nelson, 2003). The third stage of the PV effect is referred to as the charge separation at the *p*-*n* junction.

A solar cell usually consists of *p*- and *n*-type layers, where the *p*-type layer contains more charged holes as the majority carrier while the *n*-type layer contains more electrons as the majority carrier. As *p*- and *n*-type layers are bonded together, the diffusion between the charge carriers from a region of a higher concentration to a lower concentration occurs until an equilibrium state is achieved. Holes move from the *p*-layer to the *n*-layer, while electrons move from the *n*-layer to the *p*-layer. As the charge equilibrium state is achieved at the *p*-*n* junction, a depletion region is formed as shown in Figure 1.2, where the negative charges are at the *p*-layer and the positive charges are at the *n*-layer near the junction to form a charge equilibrium state. The diffusion of charges created an electric field in the depletion zone, where the electrons are driven towards the *n*-type side while the holes move towards the *p*-type side after the electron-hole separation (Smets *et al.*, 2016). The fourth stage of the PV effect is the potential

difference creation, where the charge imbalance between *n*-type and *p*-type sides creates a potential difference (voltage) across the cell. Under open-circuit conditions, the potential difference refers to the open-circuit voltage. The last stage of the PV effect is the current generation and electricity flow. When an external circuit is connected to the solar cell, the movement of electrons and holes in the circuit, caused by the potential difference between *n*-type and *p*-type sides, creates an electric current, which can be used for electric appliances.

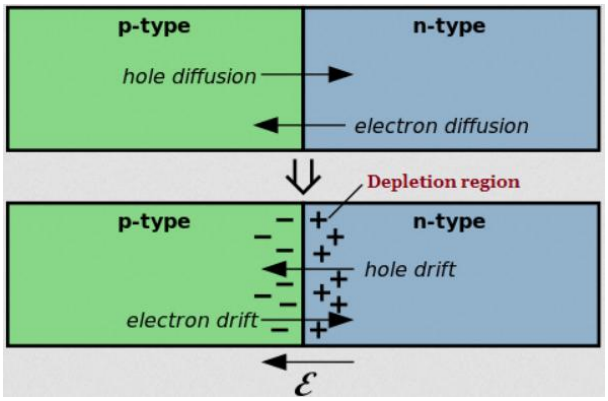

Figure 1.2: Hole-electron diffusion at *p*-*n* junction and electric field formation at the depletion zone (Nelson, 2003)

Solar cells can be classified based on technological progress, where the first generation is often the silicon-based solar cell, while the second and third generations refer to the semiconductor compound and emerging novel-based solar cells, respectively. The solar cell technology is summarized in Figure 1.3. The silicon-based solar cell consists of crystalline and amorphous types with thick material (200 – 500 μm) to absorb the photon energy due to its indirect bandgap behavior. Due to the Schockley-Quisser (SQ) limit, there is an upper limit for silicon (Si) of 29% for photon-to-electrical power conversion efficiency (PCE), where only the photons with energies

above the bandgap energy (E_g) of the material will create free electrons and holes to produce an electric current (Nayak *et al.*, 2019). The second-generation semiconductor-based solar is also known as the thin film technology with more than two (2) elements acting as the depletion zone such as group III-V and chalcogenide-based materials. III-V materials such as gallium arsenide (GaAs), indium phosphide (InP), and gallium phosphide (GaP) are often used for satellites or applications that require a high power-to-weight ratio. On the other hand, chalcogenide-based materials such as copper zinc tin sulfide (CZTS), copper indium gallium selenide (CIGS), and polycrystalline cadmium tellurium (CdTe) were developed as promising thin film materials with high flexibility and lightweight to replace silicon-based solar cells. The third-generation solar cells use emerging and novel materials such as perovskite, organic polymer, dye-sensitized photosensitive dye, graphene with a 2D honeycomb lattice structure, and perfect metamaterial absorber materials (Oni *et al.*, 2024).

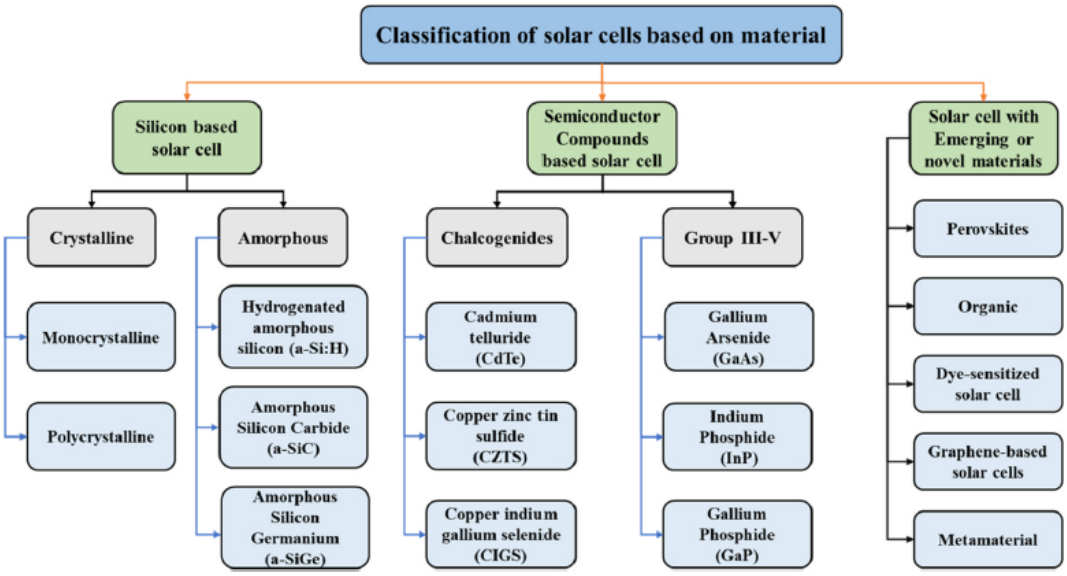

Figure 1.3: Classification of solar cells by materials (Oni *et al.*, 2024)

To date, the best research-cell efficiencies are currently maintained and benchmarked by the US National Renewable Energy Laboratory (NREL). NREL is the federal laboratory dedicated to the research, development, commercialization, and development of renewable energy, and the laboratory has been maintaining solar cell efficiency of different kinds since 1976 until mid-2025 as summarized in Figure 1.4. The chart categorized the solar cell efficiency by technologies such as crystalline silicon cells, single-junction GaAs, III-V Multijunction cells, thin film technologies, hybrid tandems, and emerging PV. Based on the latest update, the highest solar cell efficiency belonged to the III-V multijunction cells with a maximum recorded efficiency of 47.6% by a four-junction solar cell developed by Germany's Fraunhofer Institute for Solar Energy Systems. The four-junction solar cell was made of upper tandem material of gallium indium phosphide (GaInP) and aluminium gallium arsenide (AlGaAs). The upper tandem material was bonded to the lower tandem material with gallium indium arsenide phosphide (GaInAsP) and gallium indium arsenide (GaInAs). Under the single-junction GaAs category, the maximum efficiency of 30.8% was achieved by NREL under concentrated sunlight. In terms of thin-film technologies, GICS showed a maximum efficiency of 23.6%, which was developed by Evolar and Uppsala University. Perovskite and its tandem cells lead the overall emerging PV with maximum efficiencies of 26.95% and 30.1% by SoonChow University and Nanjing University, respectively. Last but not least, hybrid tandem technology also showed a promising efficiency of 36.1% under the hybridization of III-V and Si solar cells, which was developed by the Fraunhofer Institute for Solar Energy Systems and AMOLF (*Best Research-Cell Efficiency Chart*, 2025).

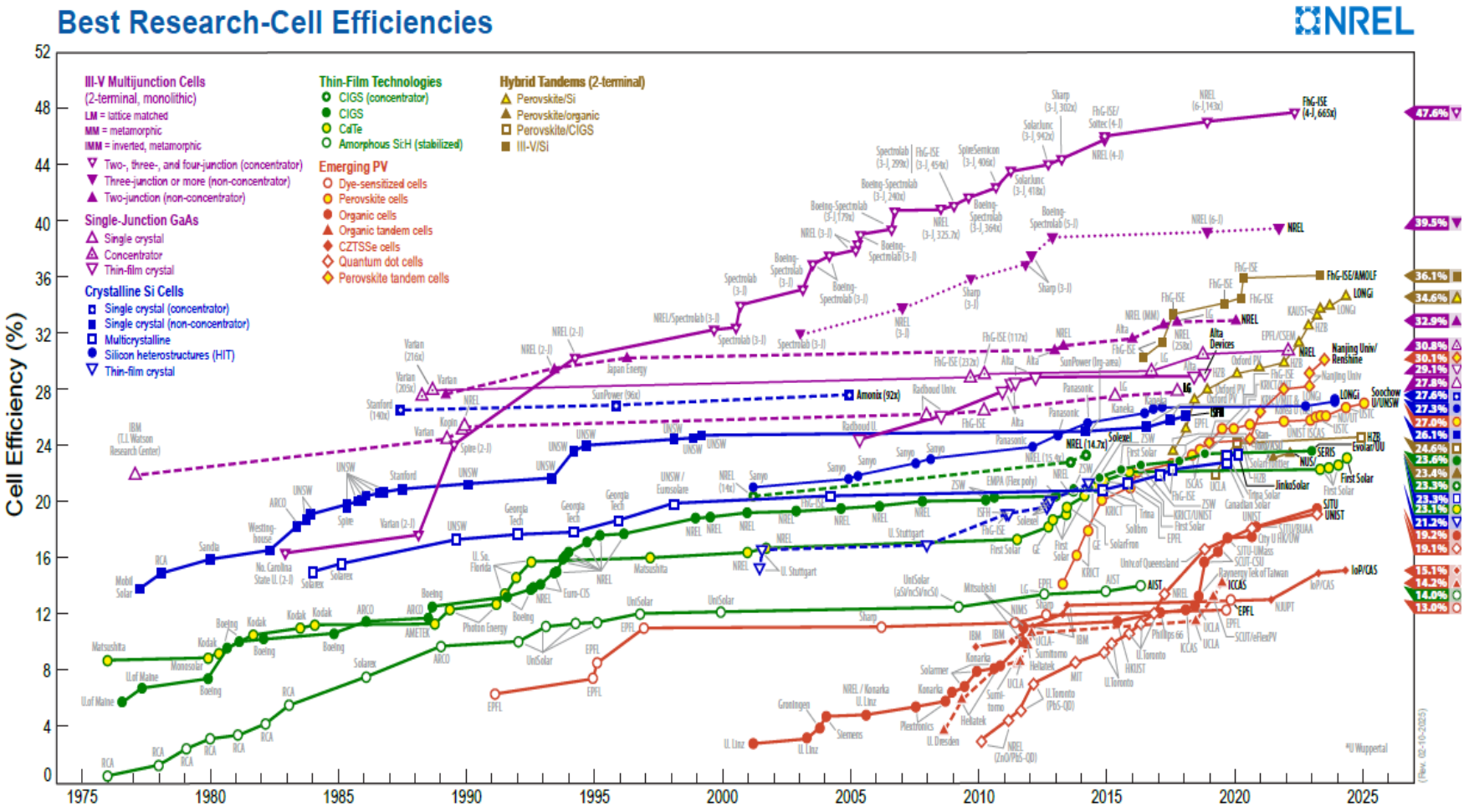

Figure 1.4: Global best research-cell efficiency chart from 1976 to 2025 (*Best Research-Cell Efficiency Chart*, 2025)

1.3 Problem statements of InGaN-based solar cell

In recent years, III-V semiconductor materials such as phosphides, arsenides, and nitrides have been heavily investigated for different optoelectronics applications such as solid-state lighting (SSL), telecommunication devices, solar cells, and high-frequency electronics. In terms of solar cell application, indium gallium nitride (InGaN) and indium alumonium nitride (InAlN) are often considered the ideal materials to harvest photon energy of the visible part of sunlight due to their tunable direct bandgap characteristics, as shown in Figure 1.5. III-V semiconductor materials, such as phosphides and arsenides, usually come with fixed bandgaps, which offer a lesser flexibility as compared to nitride alloys in maximizing the energy conversion from sunlight (Lu and Ferguson, 2013). Hence, III-V nitride alloys are ideal semiconductor materials to be tailored for solar cell applications by varying its respective composition.

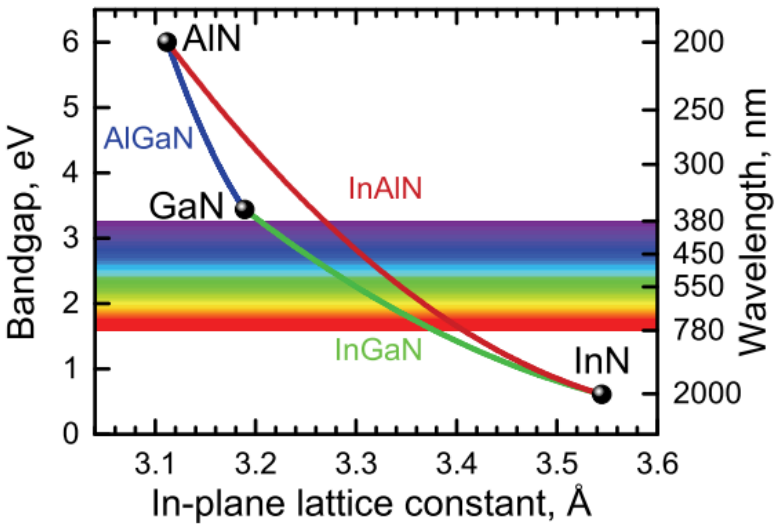

Figure 1.5: Bandgaps of wurtzite GaN, AlN, and InN and their alloys (Arteev *et al.*, 2018)

The bandgaps of InGaN and InAlN are tunable by varying their indium nitride (InN) composition. For InGaN, the bandgap varies from 0.64 eV to 3.42 eV, while for InAlN varies from 0.64 eV to 6.20 eV. Both nitride materials exhibit excellent absorption coefficients (e.g., 10^5 cm^{-1}) as compared to silicon (e.g., varied from 10^1 – 10^4 cm^{-1} with wavelength) with a wide bandgap range, and harsh environment resistance (Cañón-Bermúdez and Mulcué-Nieto, 2024). However, to maximize sunlight conversion efficiency, the bandgap of the material must be able to well-aligned with the visible light spectrum (approximately 1.65 eV to 3.10 eV), where the majority of the solar energy is concentrated with minimum energy lost due to phonon formation and heat. Next, the Burstein-Moss shift observed from the InAlN produces the variation of the bandgap for the same InN composition, which will eventually increase the bandgap of the material as the electrons at the upper edge of the valence band require greater bandgap energy to excite the empty states above the Fermi level within the conduction band (Jones *et al.*, 2008; Valdueza-Felip *et al.*, 2020). Hence, InGaN is more suitable and relatively stable than InAlN for single-junction solar cell applications to absorb peak solar irradiance in the visible light spectrum.

To fulfil the requirement of mass production and consistent output quality, the metalorganic chemical vapor deposition (MOCVD) technique has been widely used to grow InGaN/GaN thin films for different optoelectronic devices due to its relatively simple mechanism. Several challenges need to be overcome to produce InGaN-based solar cells by using this technique. The first challenge is to grow a high indium composition (>20%) InGaN thin film is high equilibrium nitrogen (N) vapor at a lower growth temperature of InGaN (< 900ºC). Due to the nature of the precursors, the partial

pressure between the III- and V-groups at different temperatures will alter the stoichiometric molar ratio of the reactant species (Chen *et al.*, 2012). Hence, the precise and accurate composition is challenging to control. At a lower growth temperature, the vapor pressure of the III-group is rather low and contributes to a lack of free energy for the pyrolysis process (Washiyama *et al.*, 2018), hence limiting the formation of nitride deposition. To grow InGaN thin films with a higher indium composition, the growth temperature must be comparatively lower to reduce the InN dissociation from its crystalline form, and also during the gas phase deposition. Nevertheless, the dissociation efficiency of ammonia (NH_3) to supply N-species will reduce at a lower growth temperature and limit the frequency for the N-species to react with the metallic indium or gallium to form InN or GaN, respectively (Stokker-Cheregi *et al.*, 2013). The insufficient N-species may cause metallic indium droplets to form at the growth front, which is inhomogeneous and contributes to bad thin film crystalline quality (Tuna *et al.*, 2011).

Next, the lack of a lattice-match substrate is another limiting factor for the growth of high crystalline quality InGaN thin film. The large lattice mismatch and thermal expansion coefficients between InN and GaN with sapphire substrate caused the compressive strain at the growth interface and led to 3D growth to achieve lattice relaxation (Sohi, Carlin, and Grandjean, 2018). The 3D growth mode due to lattice relaxation will contribute to the misfit dislocations, indium inhomogeneity, and segregation. These defects will influence the carriers' path inside the thin film, hence deteriorating the electrical performance of the devices through the alloy scattering effect (Hsu *et al.*, 2007). Due to the thermodynamic difference between InN and GaN species,

coherent 2D InGaN growth mode is limited to around an indium composition of 30% for InGaN-based devices (Lymperakis *et al.*, 2018). The thermodynamic instability between InN and GaN prompts the formation of more than one (1) phase system (e.g., phase separation), where the InGaN thin film will have different indium compositions and even with surface metallic indium segregation across the lateral growth direction (Stringfellow, 1982; Li *et al.*, 2013).

Subsequently, it is challenging to grow *p*-type InGaN thin film due to the dopant activation criteria. Magnesium (Mg) has been widely used as the *p*-type dopant in GaN and InGaN. Due to the large covalent radius of the Mg atom, the reaction between the hydrogen (H) atom and Mg forms an Mg-H complex inside the MOCVD, which makes the contact layer more passivated while causing higher electrical resistance (Cheng, 2020). Hence, Mg-H complexes limit only 1% of the electrical activity of Mg atoms present in the GaN crystal, which causes the maximum hole concentration achievable to be around 1×10^{18} cm^3 (Enatsu *et al.*, 2017). A *p*-type InGaN is crucial as the absorber layer for the *p*-*i*-*n* junction solar cell featuring a *p*-type layer, an intrinsic (*i*) layer, and a *n*-type layer structure. A *p*-*i*-*n* solar cell is often superior to a Schottky-type solar cell for several reasons, such as a wider depletion zone that enhances the electric field for electron-hole separation, reduces the recombination rate at the tunnel junction, and is more stable for large-scale production. The solar cell with a *p*-type layer as the top layer is often preferable as the minority electrons generated at the depletion zone will have higher mobility and a longer diffusion length than the holes at the *n*-layer, which allows more efficient transfer of minority carriers across the tunnel junction and reduces

recombination losses (Benigno and Darminto, 2017). Hence, the short-circuit current density and conversion efficiency of the solar cell increase.

Up-to-date, for the *p*-*i*-n homojunction InGaN-based solar cell to achieve the maximum theoretical efficiency of 23.11% (Manzoor *et al.*, 2022), an indium composition of 60% is required, which is challenging to produce with the III-V species stoichiometric complexity. Hence, re-structuring of the *p*-*i*-*n* structure is required to enhance the photon energy-capturing mechanism of the solar cell without incurring more complexity in the growth of high indium composition into the thin film. In summary, for the growth and fabrication of a functioning InGaN-based solar cell, it is crucial to understand the fundamental challenges and limitations of the current growth methodology. This understanding will pave the way for innovative solutions to overcome the aforementioned challenges. Hence, the key focus of this research work will be on the following problem statements:

a) The limited understanding of the stoichiometric relationship between growth temperature and precursor partial pressure causes the InGaN thin film to often encounter indium composition inhomogeneity, phase separation, poor crystalline quality, and defects.
b) In *p*-type InGaN for solar cells, the Mg-H complex is broken via annealing during the activation of the dopants, but the optimal annealing temperature and its subsequent impacts are still unclear.
c) The loss of photon energy through heat or phonon vibration prevents the maximum theoretical efficiency from being achieved by the current fixed

bandgap absorber design. Hence, the *p-i-n* homojunction solar cell restructuring is required to help in reducing the losses.

1.4 Research objectives

The work presented in this thesis will focus on the growth of InGaN thin films as fundamental building blocks for InGaN-based solar cells and followed by the optimization of the solar cell structure based on the fundamental properties via numerical methods. The research objectives are as follows:

a) To investigate the effects of InGaN growth temperatures (e.g., 760°C to 800°C) and precursor partial pressure (e.g., V/III ratios of 6000 to 16000) on the InGaN thin film crystalline quality by using the MOCVD technique.

b) To study the role of activation temperature (e.g., 650°C to 750°C) for the Mg-doped InGaN thin film as the *p*-layer for solar cell applications.

c) To assess the role of absorber designs (e.g, standard and graded structure), carrier concentrations (10^{16} to 10^{21} cm^{-3}), and layer thicknesses (e.g., 25 nm to 1000 nm) of the *p-i-n* homojunction InGaN solar cell via the numerical study.

1.5 The novelty of the research

The first originality of the research focuses on the stoichiometric interaction between the growth temperature and the V/III ratios as a whole instead of focusing on the single-parameter response, which could provide a holistic view of the interactive response between these two critical growth parameters. Although the annealing process will activate the Mg dopants and release holes into the thin film, the low dissociation

temperature of InN (~650°C) will limit the amount of activation heat and duration from destroying the InGaN crystalline structure. Overheating and underheating will have negative impacts on the properties of the InGaN thin film. Hence, the second originality will focus on the assessment of the activation temperature and its impact on the InGaN thin film after the annealing process, where most of the studies were focused on the activation of Mg-doped GaN. The third novelty of this study will assess the implementation of variable bandgap absorber design for the homojunction *p*-*i*-*n* InGaN solar cell as compared to the common fixed bandgap absorber design, in which the majority of the numerical studies were done.

1.6 Outline of the dissertation

Generally, the dissertation is organized as follows.

Chapter 1 is the introductory chapter, which provides a wider view of the current solar cell markets and their technology classifications. Problem statements, challenges, objectives, and novelties of this thesis.

Chapter 2 begins with a brief introduction to the InGaN characteristics and the up-to-date reported works on the MOCVD growth of InGaN thin films. The growth conditions from different literature were summarized to provide an overview of the latest growth methodology and some critical growth parameters that will impact the overall thin film quality. The theoretical overview of the *p*-*n*, *p*-*i*-n, and Schottky junction solar cells was briefed.

Chapter 3 explains the sample preparation methodology, growth conditions, devices, and other characterization details, which are further explained. The pre-conditions of the numerical study are further elaborated on the formation of the simulation model and the respective theoretical constants for the studies.

Chapter 4 discusses the characterization results of the InGaN thin film by evaluating the optical, electrical, morphological, and structural properties of the InGaN thin films grown under different temperatures. The results will be investigated and explained in detail. The chapter also summarized the key findings, which served as the foundation for the subsequent research studies.

Chapter 5 discusses the characterization results of the InGaN thin films by evaluating the optical, electrical, morphological, and structural properties of the InGaN thin films grown under different V/III ratios. The interaction between the indium composition, crystalline quality, and carrier concentration with the V/III ratios was elaborated.

Chapter 6 discusses the characterization results of InGaN thin films with highly doped magnesium (Mg). The Mg-doped InGaN thin films were annealed at different temperatures. The respective structural, electrical, and morphological properties are further discussed. The failure to get *p*-type behavior is elaborated, which may provide insight into future samples' growth with *p*-type behavior.

Chapter 7 discusses the results of numerical studies with the use of the indium composition of InGaN thin film from the experimental data. The optimum doping level and InGaN solar cell structure will be proposed as the foundation for device fabrication in the future.

Chapter 8 draws the conclusion and future recommendations with the lessons learned from the studies conducted, as well as some insights to move the topic further toward the realization of the actual solar cell devices.

CHAPTER 2 LITERATURE REVIEW

2.1 Overview of literature review

In this chapter, the properties of the InGaN will first be reviewed, followed by current epitaxial growth methodology and a details explanation of the MOCVD processes. Next, the content will be elaborated on the current MOCVD growth under different parameters and Mg-doped InGaN thin films. The respective lessons learnt will be summarized as a short remark, which serve as crucial information for the subsequent studies. In the last part of the chapter, the basics of the Schottky and homojunction *p-n* junctions will be briefed together with the up-to-date numerical studies results.

2.2 Indium gallium nitride (InGaN) and its properties

InGaN is a ternary compound made up of indium (In), gallium (Ga), and nitrogen (N) elements. A wide range of bandgap energies could be produced by adjusting the indium composition, making it a remarkable material for diverse applications such as light-emitting diodes (LEDs), light amplification by stimulated emission of radiation (LASER) diodes, radio frequency (RF) transistors, and power devices. The extreme radiation resistance from InN makes InGaN a suitable solar cell material for long space missions (Podlipskas *et al.*, 2019).

The bandgap energies vary from near-infrared (InN ~0.64 eV) to ultraviolet (GaN ~3.42 eV) spectral regions, making it an attractive material to match the entire air-mass-1.5 solar spectrum. For a homojunction *p-i-n* InGaN solar cell to perform at its maximum potential, the required bandgap energy should be ~1.4 eV, where this is

the balance point between photon absorption and voltage output, as aligned with the Shockley-Queisser limit of the silicon-based solar cell from 26.1% to 33.0% (Manzoor *et al.*, 2021, Zanatta, 2022). For the maximum homojunction InGaN solar cell performance, the estimated indium composition required is around ~60%. However, the growth of an InGaN thin film with ~60% is extremely challenging, as elaborated in Chapter 1. The theoretical bandgap energies of wurtzite GaN, InN, and their respective alloys can be derived with Vegard's law and distributed as shown in Figure 2.1, and photoluminescence (PL) intensities are arbitrary values with no relevance. As the indium composition increases, the bandgap energy of the InGaN will be redshifted to a longer wavelength close to the near-infrared region, while reducing the indium composition will move the wavelength shorter to the ultraviolet region. As the indium composition increases, the effect of thermal and alloy broadening and other mechanisms will widen the PL spectra, especially the indium composition of ~40% – 60% (Arteev *et al.*, 2018).

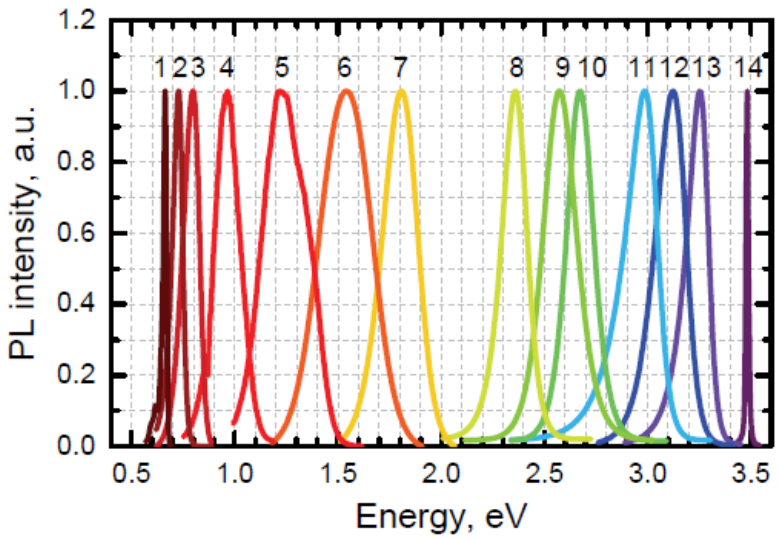

Figure 2.1: Normalized PL spectra of InGaN alloys at 77K with indium composition of (1) 100%; (2) 95%; (3) 89%; (4) 67%; (5) 50%; (6) 40%; (7) 34%; (8) 21%; (9) 17%; (10) 13%; (11) 10%; (12) 3.5%; (13) 2%; (4) 0% (Arteev *et al.*, 2018)

The properties of the InGaN alloy can be derived through the empirical rule known as Vegard's law. The law stated that the properties of the solid alloy vary linearly with its composition, with the assumption that the material has a similar crystal structure. For GaN and InN with a wurtzite crystal structure, the properties of the InGaN can be linearly interpolated from its source nitride compounds. Critical properties such as lattice constants, electron effective mass at the band edge, and electron mobility of InN and GaN are listed in Table 2.1.

Table 2.1: Material properties of wurtzite bulk GaN and InN (Chen, Ji, and Lau, 2020)

Parameter	GaN	InN
Crystal structure	Wurtzite	Wurtzite
Bandgap, E_g (T = 0K) (eV)	3.51	0.69
Bandgap, E_g (T = 300) (eV)	3.42	0.64
Lattice constant *a* (T = 300K) nm	0.3189	0.3533
Lattice constant *c* (T = 300K) nm	0.5185	0.5693
Coefficient of thermal expansion $\Delta a/a$ (10^{-6}/K)	5.6	3.8
Coefficient of thermal expansion $\Delta c/c$ (10^{-6}/K)	3.2	2.9
Melting point (ºC)	2791	2146
Static dielectric constant ($\varepsilon_S/\varepsilon_o$)	8.9	10.5
High-frequency dielectric constant ($\varepsilon_\infty/\varepsilon_o$)	5.4	6.7
Exciton binding energy (meV)	34	9
Exciton Bohr radius (nm)	2.4	8
Electron effective mass at band edge m^*_e/m_o	0.20	0.07
Electron mobility (t = 300K) cm^2/Vs	900	4400
A_1 (TO) phonon (cm^{-1})	532	447
A_1 (LO) phonon (cm^{-1})	734	586
E_1 (LO) phonon (cm^{-1})	741	593
E_1 (TO) phonon (cm^{-1})	559	476
E_2 (High) phonon (cm^{-1})	568	488
E_2 (Low) phonon (cm^{-1})	144	87

The bandgap energy of the InGaN can be calculated according to modified Vegard's Law with a bowing factor (*b*) to account for the non-linear bandgap behavior

of InGaN, and the relationship between the bandgap and the indium composition can be described below:

$$E_g(In_xGa_{1-x}N) = x.E_g^{InN} + (1-x).E_g^{GaN} - b.x.(1-x) \quad (2.1)$$

where E_g^{InN} and E_g^{GaN} are the bandgap energies of InN and GaN, respectively; b is the bowing factor equal to 1.43 eV (Wu *et al.*, 2002) and x is the ratio of indium composition.

2.3 Epitaxial growth and metalorganic chemical vapor deposition (MOCVD) technique

To grow a high-crystalline-quality InGaN thin film, the basic principle of epitaxial growth must be understood. The epitaxial process is defined as the crystal growth method where new crystalline layers are formed in the order of the crystalline orientation of a growing substrate. Epitaxial growth comes from the word *Epitaxy*. "Epi" means above and "Taxy" means ordered and layer-by-layer, which indicates the growing process involves the material deposition on top of a given substrate in an ordered and layer-by-layer manner. If the deposition of the material is of the same chemical composition as the substrate (e.g., GaN on GaN template), then it is known as homoepitaxy; otherwise, it will be known as heteroepitaxy (GaN on Sapphire substrate) (Sumanth Kumar, Jai Kumar, and Mahesh, 2018). In the past few decades, several epitaxial methods such as liquid-phase epitaxy (LPE), chloride vapor phase epitaxy (CIVPE), hydride vapor phase epitaxy (HVPE), molecular beam epitaxy (MBE), and metal-organic chemical vapor deposition (MOCVD) have been developed. Their advantages and disadvantages as summarized in Table 2.2.

Table 2.2: Overview of epitaxial growth techniques (Biefeld, Koleske and Cederberg, 2015)

Technique	Advantage	Disadvantage
LPE	• Simple mechanism (e.g., substrate contacts with molten material) • No vacuum and complex gas delivery system is required	• Available for research scale and not cost economics
CIVPE	• Simple mechanism (e.g., a hot-wall quartz reactor with a multizone furnace equipped with a basic gas delivery system. • No vacuum and complex gas delivery system is required	• Not support aluminium (Al) and antimony (Sb)
HVPE	• Well-developed and able to support large-scale • High growth rate of 10-100 μm/hr as compared to MOCVD (1-10 μm/hr) and MBE (< 1 μm/hr)	• Does not support aluminium (Al) and antimony (Sb) • Hazardous precursors
MBE	• Uniform material deposition (e.g., monolayer control) • Abrupt growth interfaces • *In-situ* monitoring for precise control	• Difficult to grow phosphide and arsenide material • Low output and longer downtime are required for maintenance • A vacuum and a complex gas delivery system are required
MOCVD	• Abrupt growth interface • Robust process and reactor structures are relatively simpler • Available on a large scale (e.g., cost-effective) • *In-situ* monitoring for precise control	• Expensive reactants • Hazardous precursors • A vacuum and a complex gas delivery system is required.

By comparing different growth techniques, epitaxial growth techniques such as LPE, CIVPE, and HVPE are deemed to be not suitable for the solar cell application due to their limited scalability, material deposition thickness uniformity, poor control over the complex growth process, and limited material selection. On the other hand, MBE and MOCVD are both suitable for solar applications due to their abrupt growth and *In-situ* precision control system. However, the MOCVD technique is a more suitable method for this study to process a larger substrate to obtain a bigger solar cell wafer. Therefore, more photon energy can be converted to electrical energy at a relatively cheaper cost as compared to the MBE technique. Different types of MOCVD technologies for mass production have been developed, such as State-of-the-art Planetary deposition from Aixtron, Germany, and TurboDisc rotating disc deposition from Veeco, U.S.

MOCVD technique uses chemical reactions that occur in the vapor state to deposit a solid material onto a growing substrate. Hence, this technique will be used for InGaN/GaN heterostructure samples. The reactants consist of compounds containing both metal and organic (e.g., carbon-based) components and are extremely volatile at a relatively low temperature. During the material deposition process using the MOCVD technique, a series of surface reactions such as adsorption and desorption of precursor molecules, surface adatom diffusion, and nucleation, as indicated in Figure 2.2. Adsorption involves the reaction of precursors (e.g., trimethylgallium) to their respective reactant material (e.g., NH_3) onto the substrate surface for the formation of the epitaxial layer. Desorption is a process to remove the unreacted precursors and by-products (e.g., CH_4) from the substrate surface to ensure fresh materials are always

reacting continuously for the deposition of subsequent epitaxial layers. Adatom diffusion is the migration of the reacted species across the substrate surface to the step edges at a given temperature and material flux, which are important for a smooth 2D epitaxial deposition. The aggregation of adatoms into a cluster will form a nucleation site to initiate layer-by-layer growth (Stringfellow, 1989).

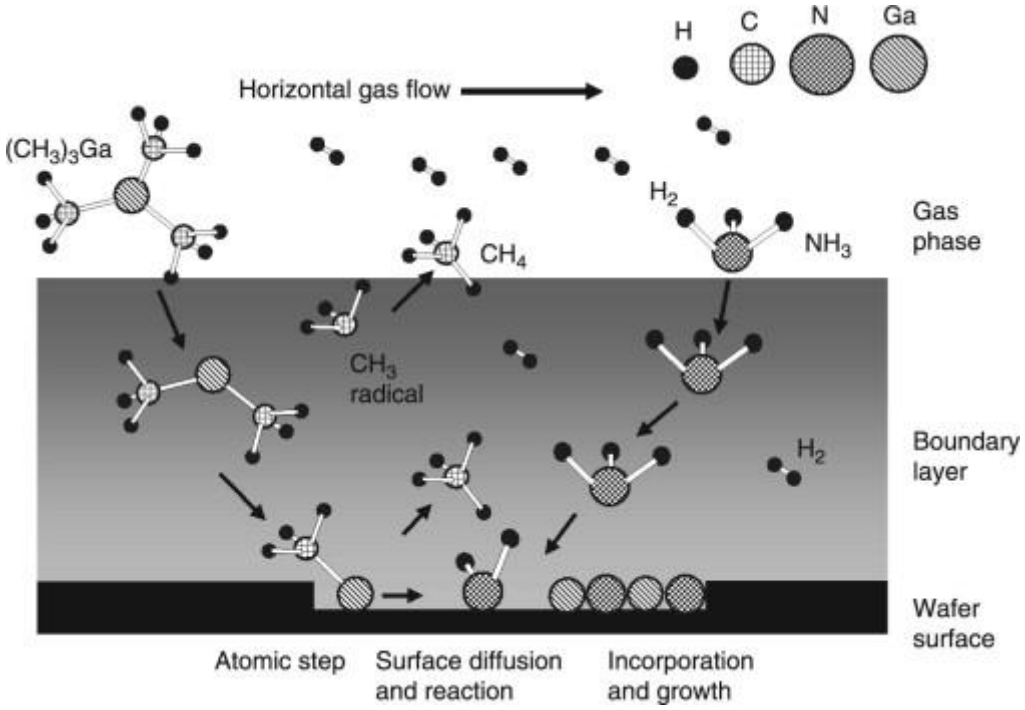

Figure 2.2: Chemical reactions during the MOCVD process (Yang, 2014).

2.4 Growth of InGaN thin films of different indium compositions and V/III ratios

To study the stoichiometric relationship between the InGaN growth parameters as defined in the research objectives, the fundamental growth limitation must be well understood before designing a design of experiment (DoE) to scope down the best performance parameters. First of all, the miscibility gap between InN and GaN results